Effect of cesium additions on lasing characteristics of copper vapor laser

A.M. Boichenko,[1] G.S. Evtushenko,[2,3] O.V. Zhdaneev,[2,3] and S.I. Yakovlenko[1]

[1] Institute of General Physics, Russian Academy of Sciences, Moscow
[2] Tomsk Polytechnic University
[3] Institute of Atmospheric Optics,
Siberian Branch of the Russian Academy of Sciences, Tomsk

A self-consistent nonstationary kinetic model of the copper vapor laser active medium (λ = 510.6, 578.2 nm) has been constructed. The present-day experimental and theoretical facts concerning the possibility of improving the laser's generation characteristics through adding cesium atoms into its active medium are analyzed. The causes of such an improvement are revealed. New data on the laser's efficiency and output power enhancement under effect of Cs additions of optimal concentration are presented.

Introduction

Adding cesium atoms to improve power characteristics of the copper vapor laser has first been suggested by Karras (Ref. 1). However, until so far it remains unclear if the adding of cesium atoms actually improves the laser's generation characteristics. Thus, in Ref. 2, when adding the Cs admixture with the density of the order of 10^{15}–10^{16} cm^{-3}, a rise in the lasing power was observed; whereas in Ref. 3 it was reported on 1.3–1.4 time increase of the lasing power at a significantly lower densities (about 10^{13}–10^{14} cm^{-3}). Later, the effect of Cs atoms added to the active medium not of a pure copper vapor laser, but to the copper chloride vapor,[4,5] bromide vapor,[6] copper vapor, and HyBrID (Ref. 7) lasers was investigated. Nonetheless, these investigations did not give any unambiguous answer to the question on the effect of Cs additions as well. Although in some experiments[4,6,7] the lasing energy increased, in other experiments[5] no increase was observed.

The improvement of lasing characteristics was attributed in Ref. 1 to Cs atoms participation in de-excitation of metastable levels of Cu atoms. Until now, this is the most widespread viewpoint.[4–7] Nevertheless, in a series of works[3,8–10] the objections against this idea have been raised. The authors of Refs. 3 and 10 have estimated the effect of Cs additions based on simplified kinetic models and suggested some suppositions on their influence on the characteristics of copper vapor laser.

Hence, the results of the experiments conducted failed to elucidate main mechanisms of Cs influence on the copper vapor laser performance, as well as to answer the question under which conditions they may lead to improved lasing characteristics. The goal of this work is analysis of all available points of view on the problem under discussion based on calculations conducted with a detailed kinetic model of the Cu−Ne−Cs-laser active medium and elucidation of the causes of the lasing power growth due to Cs additions.

1. Description of the kinetic model

To study the effect of Cs additions on lasing characteristics of copper vapor laser, a detailed nonstationary kinetic model of the Cu−Ne−Cs active medium describing the lasing at 510.6 and 578.2 nm wavelengths has been developed. The model allows us to analyze variations of values depending on level population of Cu, Ne, and Cs atoms, their ion densities, electron temperature, and laser radiation intensity at the two wavelengths. A detailed description of the model for Cu and Ne atoms is given in Refs. 11−14. Note that, as in our earlier models, we took into account the following copper states: Cu [Cu(4 $^2S_{1/2}$), Cu($4s^2$ $^2D_{5/2}$), Cu($4s^2$ $^2D_{3/2}$), Cu(4 $^2P_{3/2}$), Cu(5 $^2S_{1/2}$)]; two levels Cu* and Cu** joining, respectively, three [Cu($^4P^0$), Cu($^4D^0$), Cu($^4F^0$)] and four [Cu($5^2P_{3/2}$), Cu($5^2P_{1/2}$), Cu($4^2D_{5/2}$), Cu($4^2D_{3/2}$)] closely located excited levels, as well as the Cu ion ground state. For Ne we considered the ground and two first excited states, Ne* (a set of 3s-levels) and Ne** (a set of 3p-levels), as well as the ground state of Ne$^+$ ion. The account of Cs additions was a novelty compared to the above-enumerated models. We took into account the ground (Cs) and four excited states of Cs atom: Cs($6P_{1/2}$), Cs($6P_{3/2}$), the level uniting two close Cs[Cs($6D_{3/2}$), Cs($6D_{5/2}$)] levels, the Cs($7S_{1/2}$) level, as well as the ground state of the Cs ion.

The model took into account the following processes with Cs participation: elastic cooling of electrons, inelastic processes (direct and stepwise ionization by electron impact, electronic excitation and de-excitation, atomic excitation and de-

excitation, resonance quenching of the copper atom metastable levels, Penning reaction), and radiative transitions (see Appendix). Probabilities of spontaneous radiative transitions $Cs(6P_{1/2})$–$Cs(6S_{1/2})$, $Cs(6P_{3/2})$–$Cs(6S_{1/2})$, and $Cs(6D)$–$Cs(6S_{1/2})$ were determined using data from Ref. 15. For transitions to the ground state, we took into account the radiation re-absorption through introduction of the escape factor (Ref. 16).

The thermal balance equation used for description of the electron temperature has in our case an additional term Q_{iCs} compared to similar equation from Refs. 11–14 that allows for the power consumed for Cs ionization. We have also introduced to the power density consumed for electron cooling due to elastic collisions with Ne atoms and Cu ions the term that accounts for the electron cooling due to elastic collisions with Cs ions.
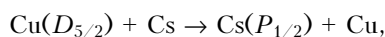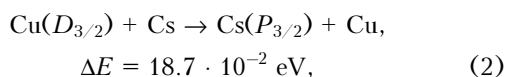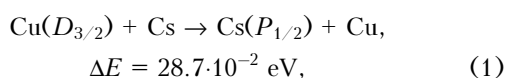
It was noted in experiments that Cs additions do not introduce significant changes in the current traversing the gas-discharge tube (GDT), therefore, we used one and the same time dependence of the current for all densities, in describing the current density. In our calculations, we used the time dependence of the current pumping the Kulon-LT40 active element.[17]

Nonstationary self-consistent equations for densities of different reagents of the active medium and the equations of the electron thermal balance have been solved with the use of PLASER[18,19] program. To solve the stiff differential equations, Gear's algorithm was used. Total about 160 kinetic reactions were used in the model. The initial Cu density in the ground state was taken equal to $1 \cdot 10^{15}$ cm^{-3}, initial values of other reagents have been iteratively calculated in the model, i.e., after setting the initial densities of reagents, their values by the beginning of the next pulse were calculated. The iterations terminated at the difference between the initial and resulting values less than 1%.
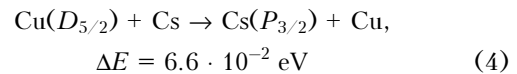
2. Supposed mechanisms of the Cs addition effect on the Cu vapor laser characteristics and their analysis

In this section, supposed mechanisms of the Cs addition influence on the Cu-vapor laser generation characteristics are sequentially outlined.

1. The authors of recent experimental study of the Cs influence on the Cu-vapor laser characteristics[4,6,7] considered the Cs atoms as the acceptors of the energy from the Cu atoms in metastable states in the processes:

$$Cu(D_{3/2}) + Cs \rightarrow Cs(P_{1/2}) + Cu,$$
$$\Delta E = 28.7 \cdot 10^{-2} \text{ eV}, \qquad (1)$$

$$Cu(D_{3/2}) + Cs \rightarrow Cs(P_{3/2}) + Cu,$$
$$\Delta E = 18.7 \cdot 10^{-2} \text{ eV}, \qquad (2)$$

$$Cu(D_{5/2}) + Cs \rightarrow Cs(P_{1/2}) + Cu,$$

$$\Delta E = 0.6 \cdot 10^{-2} \text{ eV}, \qquad (3)$$

$$Cu(D_{5/2}) + Cs \rightarrow Cs(P_{3/2}) + Cu,$$
$$\Delta E = 6.6 \cdot 10^{-2} \text{ eV} \qquad (4)$$

and provide for faster quenching of their metastable states in the afterglow. However, this point of view is not generally accepted. The estimates[8–10] have shown that this mechanism under conditions of the Cu-vapor laser operation can not explain the observed improvement[3,4,6,7] of laser characteristics, because the relaxation time for (1)–(4) reactions at the given Cs densities exceeds by several times the interpulse gap.

In fact, this time can be estimated as $\tau = [N_{Cs} \cdot \langle \sigma v \rangle]^{-1}$, where N_{Cs} is the Cs atom density; σ is the cross section of the excitation transfer at the interaction of Cs and Cu atoms; v is the relative speed of Cs atoms. For almost resonance processes of (1) – (4) type the cross section can be estimated to be $\sigma = 1 \cdot 10^{-15}$ cm^2 (Ref. 16). At $N_{Cs} = 1 \cdot 10^{12}$ cm^{-3} corresponding to optimal (in terms of maximum energy generation) Cs atom densities[4,6,7] and $v = 1 \cdot 10^5$ cm/s, $\tau = 10$ ms.

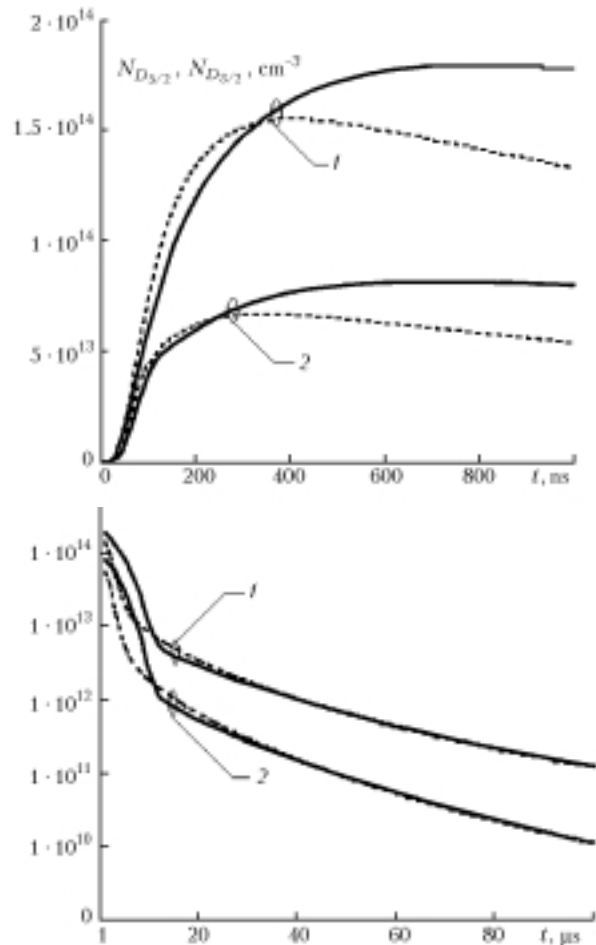**Fig. 1.** Time dependences of population for $D_{5/2}$ (1) and $D_{3/2}$ (2) levels (solid line: $N_{Cs} = 0\%$; dotted line: $N_{Cs} = 1 \cdot 10^{14}$ cm^{-3}).

Table. The initial values of plasma reagents at 10 kHz repetition frequency of the excitation pulses

Reagent	$N_{Cs} = 0$, cm^{-3}	$N_{Cs} = 1 \cdot 10^{12}$, cm^{-3}	$N_{Cs} = 1 \cdot 10^{13}$, cm^{-3}	$N_{Cs} = 5 \cdot 10^{13}$, cm^{-3}	$N_{Cs} = 1 \cdot 10^{14}$, cm^{-3}	$N_{Cs} = 5 \cdot 10^{14}$, cm^{-3}
$Cu^+ + Ne^+$	$1.086 \cdot 10^{13}$	$1.083 \cdot 10^{13}$	$1.057 \cdot 10^{13}$	$9.32 \cdot 10^{12}$	$7.4 \cdot 10^{12}$	$1.29 \cdot 10^{11}$
$Cu_{D_{5/2}}$	$1.19 \cdot 10^{11}$	$1.18 \cdot 10^{11}$	$1.18 \cdot 10^{11}$	$1.15 \cdot 10^{11}$	$1.15 \cdot 10^{11}$	$1.01 \cdot 10^{11}$
$Cu_{D_{3/2}}$	$1.11 \cdot 10^{10}$	$1.1 \cdot 10^{10}$	$1.09 \cdot 10^{10}$	$1.06 \cdot 10^{10}$	$1.06 \cdot 10^{10}$	$9.93 \cdot 10^{9}$
$Cs_{P_{1/2}}$	–	$2.52 \cdot 10^{7}$	$2.5 \cdot 10^{8}$	$1.28 \cdot 10^{9}$	$2.87 \cdot 10^{9}$	$1.84 \cdot 10^{10}$
$Cs_{P_{3/2}}$	–	$3.28 \cdot 10^{7}$	$3.25 \cdot 10^{8}$	$1.68 \cdot 10^{9}$	$3.82 \cdot 10^{9}$	$2.5 \cdot 10^{10}$
Cs_D	–	$1.63 \cdot 10^{6}$	$1.65 \cdot 10^{7}$	$9.28 \cdot 10^{7}$	$2.26 \cdot 10^{8}$	$6.26 \cdot 10^{8}$
$Cs_{7S_{1/2}}$	–	$6.77 \cdot 10^{5}$	$6.86 \cdot 10^{6}$	$3.89 \cdot 10^{7}$	$9.64 \cdot 10^{7}$	$3.4 \cdot 10^{8}$
Cs^+	–	$7.69 \cdot 10^{9}$	$7.89 \cdot 10^{10}$	$4.79 \cdot 10^{11}$	$1.35 \cdot 10^{12}$	$7.11 \cdot 10^{12}$
Cs	–	$9.93 \cdot 10^{11}$	$9.86 \cdot 10^{12}$	$4.93 \cdot 10^{13}$	$9.87 \cdot 10^{13}$	$4.85 \cdot 10^{14}$
T_e	0.147	0.147	0.146	0.146	0.146	0.15
E_{510}, J/cm^3	$6.36 \cdot 10^{-6}$	$6.34 \cdot 10^{-6}$	$6.3 \cdot 10^{-6}$	$6.1 \cdot 10^{-6}$	$5.62 \cdot 10^{-6}$	$9.34 \cdot 10^{-7}$
E_{578}, J/cm^3	$2.96 \cdot 10^{-6}$	$2.96 \cdot 10^{-6}$	$2.88 \cdot 10^{-6}$	$2.7 \cdot 10^{-6}$	$2.4 \cdot 10^{-6}$	0
E_t, J/cm^3	$9.32 \cdot 10^{-6}$	$9.3 \cdot 10^{-6}$	$9.18 \cdot 10^{-6}$	$8.8 \cdot 10^{-6}$	$8.02 \cdot 10^{-6}$	$9.34 \cdot 10^{-7}$
E_{kor}, J/cm^3	$9.32 \cdot 10^{-6}$	$9.323 \cdot 10^{-6}$	$9.495 \cdot 10^{-6}$	$10.612 \cdot 10^{-6}$	$11.204 \cdot 10^{-6}$	$3.571 \cdot 10^{-7}$
P_{kor}, W	35.136	35.147	35.795	40.006	42.238	1.346

N o t e : The initial values the plasma reagents parameters have been obtained by self-consistent calculation (see Sect. 1 for the description of the model). E_t is the total specific energy of lasing; E_{510} is the specific energy of lasing at 510.6 nm wavelength; E_{578} is the specific energy of lasing at 578.2 nm wavelength; P_{kor} is the mean lasing power at a constant efficiency of lasing. The gas discharge tube had the parameters presented in Ref. 17: 120-cm length, the inner radius of 1 cm, and concentration of the buffer gas of $4 \cdot 10^{17}$ cm^{-3}.

Optimal frequency of the excitation pulse repetition is about 10–20 kHz, that corresponds to the interpulse gap of 0.1 ms as long, which is two orders of magnitude shorter than τ. The influence of these reactions in the active medium is illustrated by the results calculated using the above scheme shown in Fig. 1, which shows the curves both taking into account and ignoring the (1)–(4) reactions. It is seen that the reactions of the excitation resonance transfer from Cu atom metastable levels do not affect significantly their time dependence. In particular, starting from about 10 μs, the curves virtually coincide. The GDT parameters and the plasma reagent values used in the calculations are given in the Table.

The study by Belokrinitskii et al. (Ref. 3) is presumably the most thorough present-day theoretical study of the effect of Cs additions on the Cu-vapor laser characteristics. In this study, several causes are outlined of possible positive influence of the Cs additions on generation characteristics of the laser.

However, some simplifying suppositions used there could affect somehow the work's conclusions. It is interesting to analyze them using a more detailed model. Therefore, in our analysis, we shall consider in a more detail the Cs addition influence.

2. The viewpoint is outlined in Ref. 3 that in the presence of Cs admixture the interpulse relaxation of the electron gas temperature proceeds faster than for Cu–Ne active medium. The authors attribute this effect to some additional mechanism of cooling electrons in collisions with Cs atoms.

The cooling time in Coulomb electron collisions can be estimated by the following relations[10]:

$$\tau_{gas} \cong \left(2\nu_{ei} \frac{m_e}{M_i} \right)^{-1}, \qquad (5)$$

$$\nu_{ei} = \frac{4\sqrt{3}}{9} \pi \frac{e^4 N_e \ln \Lambda_k}{m_e^{1/2} T_e^{3/2}} \cong 5.076 \cdot 10^{-6} \frac{N_e \ln \Lambda_k}{\sqrt{T_e^3}},$$

where m_e is the electron mass; ν_{ei} is the frequency of the Coulomb electron-ion collisions; $\ln\Lambda_k$ is the Coulomb logarithm (≈ 10). It is supposed in the latter formula that the electron density is given in cm^{-3}, the electron temperature in eV, and the frequency in s^{-1}. Under standard excitation conditions (generation power is of the order of several tens of watts and the tube radius is about 1 cm), the characteristic values of electron density in the beginning of the interpulse period (several microseconds after the beginning of the excitation pulse) are about $5 \cdot 10^{13}$ cm^{-3} and the electron temperature is 0.5 eV. Under the laser operation described in Refs. 4, 6, 7, where optimal density of the Cs admixture was 10^{12} cm^{-3}, the cooling time in the Coulomb electron-ion collisions decreased by less than 2% even assuming that all Cs atoms were ionized. Under laser operation conditions from Ref. 3, the optimal Cs density was about several units multiplied by 10^{13} cm^{-3}. Substitution of the additional electron density corresponding to this value into Eq. (1) will decrease the relaxation time

by 17.5%. However, our calculations show the electron density value at adding the Cs admixture to exceed this value for pure copper only in the very beginning of the afterglow (for more detail see Section 3). In the presence of Cs additions in the active medium, the drop of the electron density occurs faster and it results in a lower pre-pulse electron densities (this coincides with conclusions of Ref. 10; also see Section 3). Thus, as calculations show, in fact the relaxation time does not decrease and even can increase. In other words, the increase of electron density in the case of the laser with Cs additions is of a short-term character.

3. In Ref. 3, a more rapid reconcentration of Cu atoms in the ground state before the beginning of the excitation pulse at a simultaneous increase of the relaxation speed of populating the metastable states was noted. The authors of Ref. 3 explain this fact by a higher density of electrons in the period between the pulses and their lower temperature at the very end of the afterglow. However, they do not explain the mechanisms through which the higher electron density during the afterglow and the lower electron temperature at the end of the interpulse period can

result in a higher reconcentration of Cu atoms in the ground state.

Results of our modeling confirm the fact of a lesser exhaustion of Cu atom ground level during the excitation pulse in the presence of Cs atoms. Let us discuss this conclusion in a more detail. First, in our calculations during the entire interpulse period the electron density with the Cs additions does not exceed the electron density free of them (see Subsection 2.2). The lower degree of exhaustion is due to a lower energy deposition into the discharge. After termination of the excitation pulse, due to intense recombination of Cu ions, somewhat more intense reconcentration of Cu atoms in the ground state is observed. However, when the afterglow starts (approximately, starting from the 2nd microsecond, Fig. 2), the rates of reconcentration are practically equal in the both cases, because in the active medium with Cs the temperature of electrons is a bit lower, as well as their density (Figs. 3 and 4). Our analysis of the Cu atom ground state exhaustion has shown that plasmochemical reactions with the participation of Cs atoms do not affect immediately the ground state population.
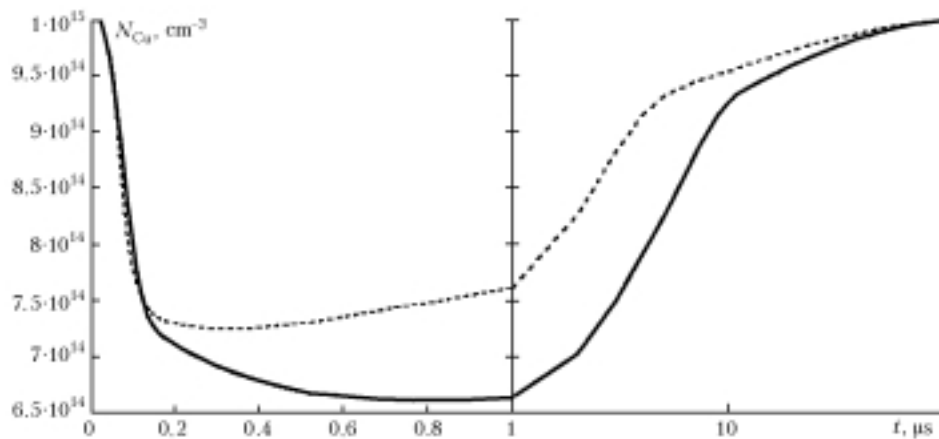
Fig. 2. Time dependences of Cu atom density in the ground state during the excitation pulse and in the interpulse period (solid line: $N_{Cs} = 0\%$; dotted line: $N_{Cs} = 1 \cdot 10^{14}$ cm^{-3}).
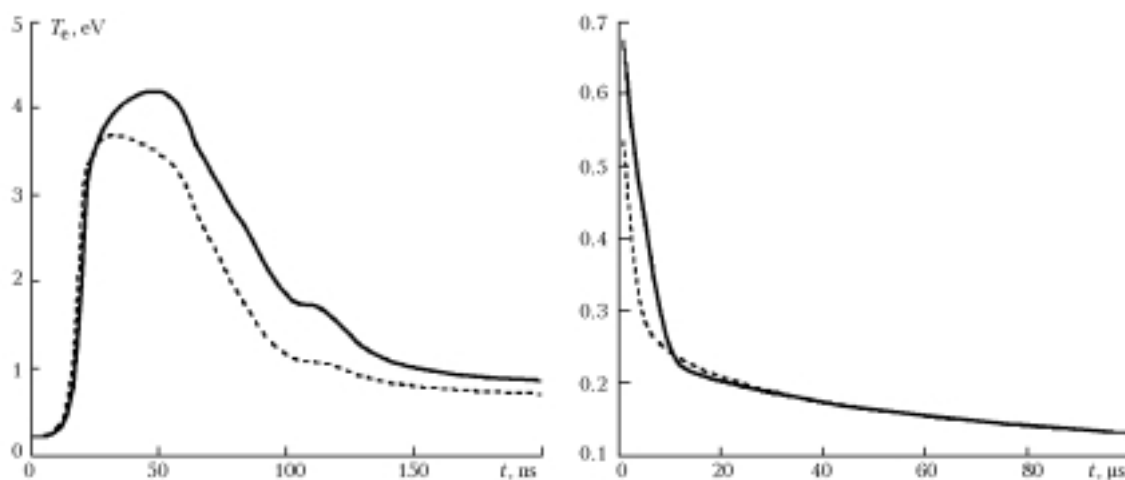
Fig. 3. Time dependences of the electron temperature during the excitation pulse and in the interpulse period (solid line: $N_{Cs} = 0\%$; dotted line: $N_{Cs} = 1 \cdot 10^{14}$ cm^{-3}).
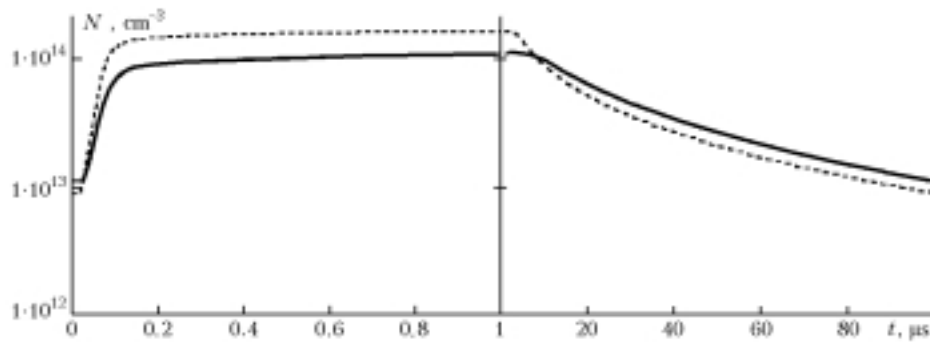
Fig. 4. Time dependences of the electron density during the excitation pulse and in the interpulse period (solid line: $N_{Cs} = 0$%; dotted line: $N_{Cs} = 1 \cdot 10^{14}$ cm^{-3}).

4. The modeling results from Ref. 3 show that an excess of optimal density of the Cs atoms results in elevation of the pre-pulse density of Cu atoms in the metastable state.

The calculated results obtained using our kinetic model contradict these conclusions. In our calculations, the pre-pulse density of Cu atoms in metastable states does not raise at any densities of Cs atoms (see Table). In adding Cs, the pre-pulse population of the Cu atom metastable levels steadily falls down due to both lower relaxation during the pumping pulse (see Fig. 1 and Subsections 2.3, 2.7) and a decrease of the pre-pulse electron temperature. The electron temperature decreases, because the Cu atom density in the metastable states tends to equilibrium. Our analysis of population dynamics for the $D_{5/2}$ metastable level shows that the Cs admixture does not affect density of Cu atoms in the metastable states neither during the pump pulse, nor in the afterglow (Fig. 1). Noticeable pre-pulse fall of the density of Cu atoms in the metastable states takes place, if the amount of Cs admixed approaches some critical value, at which the lasing breaks (see Table).

5. As noted in Ref. 3, the pre-pulse electron density does not affect the lasing power, although the authors did not substantiate this supposition.

The pre-pulse densities of the active medium reagents may change because of their insufficient relaxation between the pulses, for example, at increasing frequency of the excitation pulse repetition or for different active admixtures. It was shown[11,12,20–24] that the pre-pulse density of electrons makes an immediate effect on lasing characteristics of Cu-vapor laser. According to our calculations, in the presence of Cs atoms in the active medium the lasing characteristics depend on the pre-pulse density of electrons as well.

6. According to Ref. 3, it was experimentally established that the Cs admixtures cause a decrease of time for the development of a discharge and simultaneous increase of the rate of pulse rise and a decrease of its amplitude.

Our calculations gave the same result. Acceleration of discharge development in the laser plasma in the presence of Cs admixture is explained by a faster enhancement of the electron density (development of electron avalanche) due to a lower

ionization potential of Cs atom. Thus, in applying the excitation pulse, the gas ionization in the active medium starts earlier, and this provides a decrease of the rate of excitation pulse rise.

7. A reduction of the plasma active resistance was noted experimentally at adding Cs.[3]

Our model confirms such a behavior of the resistance. Optimal density of Cs additions does not exceed several units multiplied by 10^{13} cm^{-3}, in our calculations it does not exceed 10^{14} cm^{-3}. At such densities, the contribution of the electron–atom collisions to the plasma conductivity is insignificant (the cross section of electron scattering by Cs atoms is in maximum about 600 Å); therefore, in modeling the Cu-vapor laser with Cs additions we used the corresponding expression for specific resistance from Refs. 11–14. Thus, Cs admixtures indirectly affect variations of plasma resistance of the Cu-vapor laser through variations of time dependences of the electron density and temperature (see Section 3). Because of the lower pre-pulse density of electrons, the pre-pulse plasma resistance with Cs additions is higher (see Section 3), however, fast rise of the electron density provides a more sharp fall off of the resistance during the first tens nanoseconds, that results in lowering the energy entering the discharge and, correspondingly, in the improved efficiency.

8. It is stated in Refs. 9 and 10 that adding Cs admixtures to active medium leads to lowering of the electron temperature because of reduction of the energy consumed for ionization and decrease of recombination heating at the afterglow stage.

Actually, the energy entering a discharge significantly decreases at adding Cs admixtures due to enhancement of the electron density during the excitation pulse. This results in a reduction of the plasma resistance and, correspondingly, of the input energy (see Subsection 2.7). It should be noted that the lasing break in the presence of cesium in the active medium corresponds to a higher temperature of electrons than in its absence. Thus, for the current used in our model (see Section 3) the electron temperature corresponding to the lasing break in the presence of cesium is ≈ 2.2 eV. This temperature in a pure mixture is 1.85 eV and it is close to 1.7 eV, at which the rates of excitation of resonance and metastable levels of Cu atom are comparable.

Analysis of dynamics of the plasmochemical reactions stipulates that cesium does not directly affect the electron temperature during the interpulse period.

9. It was observed in experiments[3] that a drop in voltage at the GDT accompanies adding cesium. At the same time, Refs. 4, 6, 7 present data, which show that Cs admixtures do not change noticeably the electric characteristics of the device.

Note, that it was supposed in modeling that the shape of the current pulse does not change in adding cesium (see Section 1). Variations in the plasma conductivity and voltage time shape have been discussed in Subsections 2.6 and 2.7.

3. Analysis of cesium influence on pre-pulse values and time characteristics of plasma reagents

The results of this work show that a change of Cs concentration in the laser active medium monotonically changes the pre-pulse characteristics of reagents and parameters. At the increase of Cs admixture concentration, a graduate lowering of the pre-pulse density of electrons and copper atoms in the metastable states takes place together with lowering of the pre-pulse electron temperature. Simultaneously, a growth of pre-pulse populations at all levels of the Cs atom and its ions is observed. Characteristic variations of time dependences of different plasma reagents in the active medium are shown in Figs. 1–6.
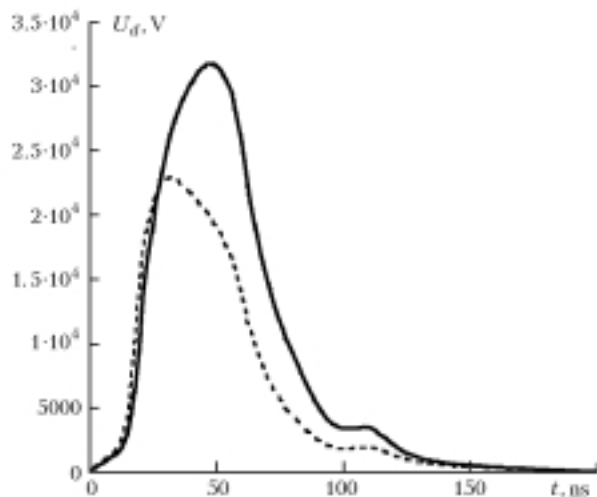

Fig. 5. Time dependence of GDT voltage; N_{Cs} = 0% (solid curve) and $1 \cdot 10^{14}$ cm^{-3} (dashed curve).

The physical processes occurring during the excitation pulse and afterglow are different, therefore, we consider these stages separately.
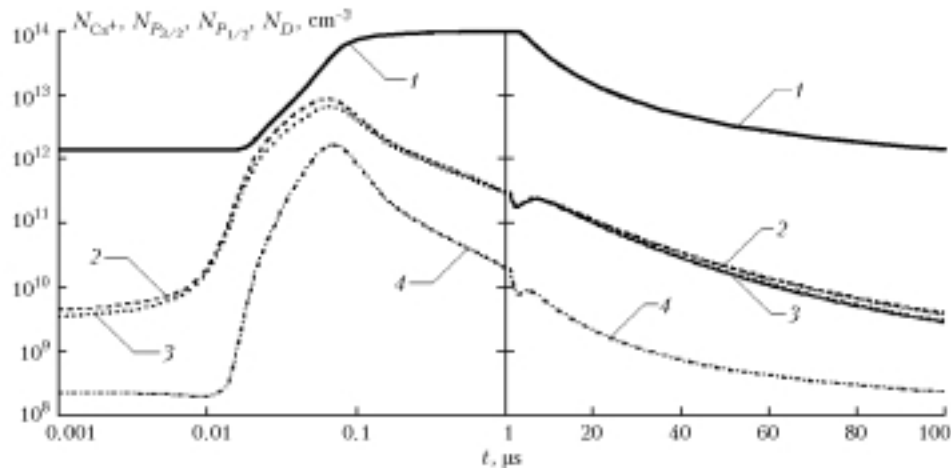
Excitation pulse

Adding Cs admixtures to the active medium leads to a drop in the voltage pulse rise time (see Fig. 5 in Subsection 2.6), and, consequently, the time of reaching the critical electron temperature, at which the excitation rates of resonance and metastable levels of Cu atom are comparable. This provides for the conditions that are more favorable for excitation of the laser active medium. A faster rise of the electron temperature due to the fall in the voltage pulse rise time results in a faster growth of the electron density. This is also favored by the fact that the ionization potential (3.89 eV) of Cs atom is much lower than that of Cu atom (7.726 eV) and especially of Ne atom (21.6 eV). Therefore, at low concentrations of cesium in the beginning of the excitation pulse its practically total ionization takes place. The rapid Cs ionization provides for the major income of electrons in the beginning of pump. The ionization and excitation of Cs atoms consumes a portion of the excitation energy.

Thus, in the beginning of the excitation pulse, less energy is spent for populating the metastable levels of Cu atom, that at optimal Cs concentrations also must favor a change of the excitation conditions in a way that favors improving lasing characteristics. Since at low energy of electrons predominantly metastable levels of Cu atom are excited, then the energy consumption for inelastic processes with Cs atoms leads to slowing the process down (see also Ref. 10). However, because of significant increase of the electron density, populations of the resonance and metastable levels in the presence of Cs additions increase faster, what determines somewhat earlier reaching of the population inversion and, consequently, of lasing. Energy consumption for inelastic processes with participation of Cs atoms and reduction of the energy income to plasma during the pump pulse results in a lowering of the maximum electron temperature and shifts the maximum to shorter times (Fig. 3). This also provides a lower depletion of the Cu atom ground state.

Interpulse period

The maximum value of the electron density in the case of adding Cs is higher than its pre-pulse value. This is explained by a higher rate of lowering the electron density. Relaxation of the electron density in the laser plasma is determined by the triple recombination. Under conditions of the active medium plasma with Cs admixture, a situation with a higher density and simultaneously a lower temperature of electrons is realized before the afterglow stage. Such a situation determines a high rate of electron recombination in the beginning of the afterglow. At the end of the afterglow a higher rate of recombination is due to a lower electron temperature. As was mentioned earlier, the resonance transfer of excitation from Cu atoms in metastable states to Cs atoms does not affect significantly the relaxation of the metastable level population (Fig. 1). Therefore, the pre-pulse density of Cu atoms in metastable states decreases only slightly with adding Cs.

Fig. 6. Time dependence of the concentration of cesium ions Cs^+ (solid curve *1*), population of the levels $Cs(P_{3/2})$ (dashed curve *2*), $Cs(P_{1/2})$ (dashed curve *3*), $Cs(D)$ (dot-and-dash curve *4*) during the excitation pulse and the interpulse interval for $N_{Cs} = 1 \cdot 10^{14}$ cm^{-3}.

The second growth of population of the resonance and metastable levels of the Cs atom in the early afterglowing at 2—5 μs (Fig. 6) is connected with the Cs ion recombination to higher atom levels. Due to lower exhaustion of population of the Cu atom ground level, it restores its pre-pulse magnitude faster, all other factors being equal. This may result in improved lasing characteristics, when operating at a high repetition frequency of the excitation pulses.

Influence of Cs additions on radiation energy

In Refs. 3, 4, 6, and 7 one can find data on the rise in the mean lasing power, laser efficiency, and optimal repetition frequency of excitation pulses. This is true both for pure Cu vapor laser,[3] Cu salt lasers, and hybrid systems.[4,6,7] Our calculations show that adding cesium results in a significant (more than 20%) enhancement of the lasing efficiency at simultaneous fall in the radiation energy. When rising Cs concentration from zero to optimum (see Table), the power pumped to the discharge decreases from 4.3 to 2.06 kW. The Cs surpassing over the optimal value results in a sharp drop in the lasing power up to its cessation (see Table). An increase in the pump current amplitude results in the lasing efficiency fall. In the presence of cesium additions, as we have just noted, the lasing efficiency grows. If the pumping current amplitude is increased so that the efficiency comes to its former magnitude (free of Cs additions), then the generation energy grows. The optimal Cs concentration increases the generation power from 35.17 W (which corresponds to 9.32 μJ/cm^3 power in a pulse) to 42.24 W (which corresponds to 11.2 μJ/cm^3 power in a pulse).

Conclusion

To address the question on the effect of Cs additions on the Cu vapor laser performance, a detailed kinetic model of Cu—Ne—Cs active medium was constructed.

A thorough analysis of the existing points of view was conducted.

It follows from the model results obtained that the presently dominating point of view on the enhancement of lasing characteristics of the Cu vapor laser with Cs additions due to resonance transfer of excitation from metastable Cu atoms to Cs atoms is faulty.

We have shown with the help of our kinetic model that adding Cs to the laser active medium results in a lowering of the pre-pulse electron density and, correspondingly, of plasma conductivity at the initial stage of the excitation pulse, which provides better coupling with the power source. Further (in several tens of nanoseconds), the electron density grows faster compared to the case without Cs, and, as a consequence, energy coming to the active medium decreases.

It is shown that adding Cs results in a more than 20% growth of the efficiency at only insignificant fall in the lasing power. This improvement is due to decrease in the energy income to the active medium after termination of the generation pulse. In its turn, this results in that at a decrease of the power contribution (for example, due to increase of the current flowing through the GDT) in such a way that the efficiency comes to its former magnitude corresponding to the absence of Cs, the mean generation power heightens by more than 20%.

In our opinion, it is most likely that the same changes will take place at adding some arbitrary easy ionized admixture.

Adding the Cs admixture results in the growth of the critical electron temperature, i.e., the temperature of the generation appearance.

It is important that there is some optimal magnitude of the Cs addition, above which deterioration of both the generation energy and efficiency occur. A particular magnitude of the Cs optimal concentration depends on GDT characteristics in a particular experiment, as well as

on the excitation pulse repetition frequency $(1 \cdot 10^{14}$ cm^{-3} for conditions of our experiment), buffer gas pressure, and other parameters.

Appendix

The following states of the Cs atom were considered: $Cs(6S_{1/2})$, $Cs(6P_{1/2})$, $Cs(6P_{3/2})$, and $Cs(7S_{1/2})$; in addition, we took into account the level joining two close excited levels $Cs(6D_{3/2})$, $Cs(6D_{5/2})$, and the Cs ion ground state. To calculate the rates of the processes Nos. 31–38, Meve's formula[16] was used; k is the constant of the reaction rate, σ is the reaction cross section, ω is the probability of spontaneous radiative transition.

Number of the process	Reaction	Rate (cross section)
1	$Cs(6P_{1/2}) + Cs(6P_{1/2}) \rightarrow Cs(6D) + Cs(6S_{1/2})$	$\sigma \sim 2 \cdot 10^{-15}$ cm^2, $k = 1.616 \cdot 10^{-10}$ cm^3/s
2	$Cs(6P_{3/2}) + Cs(6P_{1/2}) \rightarrow Cs(6D) + Cs(6S_{1/2})$	$\sigma \sim 2 \cdot 10^{-15}$ cm^2, $k = 1.616 \cdot 10^{-10}$ cm^3/s
3	$Cs(6P_{3/2}) + Cs(6P_{3/2}) \rightarrow Cs(6D) + Cs(6S_{1/2})$	$\sigma \sim 2 \cdot 10^{-15}$ cm^2, $k = 1.616 \cdot 10^{-10}$ cm^3/s
4	$Cs(6P_{1/2}) + Cs(6P_{1/2}) \rightarrow Cs(6S_{1/2}) + Cs(6S_{1/2})$	$k = 3 \cdot 10^{-9}$ cm^3/s
5	$Cs(6P_{3/2}) + Cs(6P_{1/2}) \rightarrow Cs(6S_{1/2}) + Cs(6S_{1/2})$	$k = 3 \cdot 10^{-9}$ cm^3/s
6	$Cs(6P_{3/2}) + Cs(6P_{3/2}) \rightarrow Cs(6S_{1/2}) + Cs(6S_{1/2})$	$k = 3 \cdot 10^{-9}$ cm^3/s
7	$Cs(6D) \rightarrow Cs(6S_{1/2})$	$w = 1.471 \cdot 10^7$ s^{-1}
8	$Cs(6P_{3/2}) \rightarrow Cs(6S_{1/2})$	$w = 3.732 \cdot 10^7$ s^{-1}
9	$Cs(6P_{1/2}) \rightarrow Cs(6S_{1/2})$	$w = 3.28 \cdot 10^7$ s^{-1}
10	$Cs(7S_{1/2}) \rightarrow Cs(6P_{1/2})$	$w = 5.273 \cdot 10^6$ s^{-1}
11	$Cs(7S_{1/2}) \rightarrow Cs(6P_{3/2})$	$w = 1.5 \cdot 10^5$ s^{-1}
12	$Cs(6D) \rightarrow Cs(6P_{1/2})$	$w = 1.292 \cdot 10^7$ s^{-1}
13	$Cs(6D) \rightarrow Cs(6P_{3/2})$	$w = 4.664 \cdot 10^7$ s^{-1}
14	$Cs(6D) + Cs(6S_{1/2}) \rightarrow Cs(6P_{1/2}) + Cs(6P_{1/2})$	$\sigma \sim 5 \cdot 10^{-15}$ cm^2, $k = 3 \cdot 10^{-9}$ cm^3/s
15	$Cs(6D) + Cs(6S_{1/2}) \rightarrow Cs(6P_{3/2}) + Cs(6P_{1/2})$	$\sigma \sim 5 \cdot 10^{-15}$ cm^2, $k = 3 \cdot 10^{-9}$ cm^3/s
16	$Cs(6D) + Cs(6S_{1/2}) \rightarrow Cs(6P_{3/2}) + Cs(6P_{3/2})$	$\sigma \sim 5 \cdot 10^{-15}$ cm^2, $k = 3 \cdot 10^{-9}$ cm^3/s
17	$Cs(6P_{1/2}) + Ne \rightarrow Cs(6P_{3/2}) + Ne$	$\sigma \sim 4 \cdot 10^{-16}$ cm^2, $k = 6.295 \cdot 10^{-11}$ cm^3/s
18	$Cs(6P_{3/2}) + Ne \rightarrow Cs(6P_{1/2}) + Ne$	$k = 4.22 \cdot 10^{-11}$ cm^3/s
19	$Cs(6S_{1/2}) + e \rightarrow Cs(6P_{3/2}) + e$	$k = 5 \cdot 10^{-7} \exp(-1.45/T_e) T_e^{-0.3}$ cm^3/s
20	$Cs(6P_{3/2}) + e \rightarrow Cs(6S_{1/2}) + e$	$k = 5 \cdot 10^{-7} T_e^{-0.3} \cdot 1/2$ cm^3/s
21	$Cs(6S_{1/2}) + e \rightarrow Cs(6P_{1/2}) + e$	$k = 3.55 \cdot 10^{-7} \exp(-1.39/T_e) T_e^{-0.3}$ cm^3/s
22	$Cs(6P_{1/2}) + e \rightarrow Cs(6S_{1/2}) + e$	$k = 3.55 \cdot 10^{-7} T_e^{-0.3}$ cm^3/s
23	$Cs(6S_{1/2}) + e \rightarrow Cs(6S_{1/2}) + e$	$k = 1.7 \cdot 10^{-5} \exp(-3.89/T_e) T_e^{-0.8}$ cm^3/s
24	$Cs(6S_{1/2}) + e \rightarrow Cs^+ + 2e$	$k = 1 \cdot 10^{-6} \exp(-3.89/T_e) T_e^{-0.2}$ cm^3/s
25	$Cs(6P_{1/2}) + e \rightarrow Cs^+ + 2e$	$k = 2 \cdot 10^{-6} \exp(-2.5/T_e) T_e^{-0.5}$ cm^3/s
26	$Cs(6P_{3/2}) + e \rightarrow Cs^+ + 2e$	$k = 1 \cdot 10^{-6} \exp(-2.44/T_e) T_e^{-0.3}$ cm^3/s
27	$Cs(7S_{1/2}) + e \rightarrow Cs^+ + 2e$	$k = 2 \cdot 10^{-6} \exp(-1.59/T_e) T_e^{-0.2}$ cm^3/s
28	$Cs^+ + e \rightarrow Cs(7S_{1/2}) + 2e$	$k = 5.4 \cdot 10^{-27} T_e^{-9/2}$ cm^3/s
29	$Cs(6D) + e \rightarrow Cs^+ + 2e$	$k = 3 \cdot 10^{-6} \exp(-1.11/T_e)$ cm^3/s
30	$Cs^+ + e \rightarrow Cs(6D) + 2e$	$k = 5.4 \cdot 10^{-27} T_e^{-9/2}$ cm^3/s
31	$Cs(6P_{1/2}) + e \rightarrow Cs(7S_{1/2}) + e$	$E = 0.845$ eV, $f = 0.171$, $A = 0.6$, $D = 0.28$
32	$Cs(7S_{1/2}) + e \rightarrow Cs(6P_{1/2}) + e$	$E = 0.845$ eV, $f = 0.171$, $A = 0.6$, $D = 0.28$
33	$Cs(6P_{3/2}) + e \rightarrow Cs(7S_{1/2}) + e$	$E = 0.913$ eV, $f = 0.208 \cdot 0.5$, $A = 0.6$, $D = 0.28$
34	$Cs(7S_{1/2}) + e \rightarrow Cs(6P_{3/2}) + e$	$E = 0.913$ eV, $f = 0.208$, $A = 0.6$, $D = 0.28$
35	$Cs(6P_{3/2}) + e \rightarrow Cs(6D) + e$	$E = 1.353$ eV, $f = 0.332 \cdot 0.4$, $A = 0.6$, $D = 0.28$
36	$Cs(6D) + e \rightarrow Cs(6P_{3/2}) + e$	$E = 1.353$ eV, $f = 0.208$, $A = 0.6$, $D = 0.28$
37	$Cs(6P_{1/2}) + e \rightarrow Cs(6D) + e$	$E = 1.417$ eV, $f = 0.298 \cdot 0.1$, $A = 0.6$, $D = 0.28$
38	$Cs(6D) + e \rightarrow Cs(6P_{1/2}) + e$	$E = 1.417$ eV, $f = 0.298$, $A = 0.6$, $D = 0.28$
39	$Cs + Cu(D_{5/2}) \rightarrow Cs(6P_{3/2}) + Cu$	$\sigma \sim 1 \cdot 10^{-15}$ cm^2; $k \sim 1 \cdot 10^{-10}$ cm^3/s
40	$Cs(6P_{3/2}) + Cu \rightarrow Cs + Cu(D_{5/2})$	$k \sim 6.486 \cdot 10^{-11}$ cm^3/s
41	$Cs + Cu(D_{5/2}) \rightarrow Cs(6P_{1/2}) + Cu$	$\sigma \sim 1 \cdot 10^{-15}$ cm^2; $k \sim 1 \cdot 10^{-10}$ cm^3/s
42	$Cs(6P_{1/2}) + Cu \rightarrow Cs + Cu(D_{5/2})$	$k \sim 9.833 \cdot 10^{-11}$ cm^3/s
43	$Cs + Cu(D_{3/2}) \rightarrow Cs(6P_{3/2}) + Cu$	$\sigma \sim 1 \cdot 10^{-15}$ cm^2; $k \sim 1 \cdot 10^{-10}$ cm^3/s
44	$Cs(6P_{3/2}) + Cu \rightarrow Cs + Cu(D_{3/2})$	$k \sim 2.876 \cdot 10^{-11}$ cm^3/s
45	$Cs + Cu(D_{3/2}) \rightarrow Cs(6P_{1/2}) + Cu$	$\sigma \sim 1 \cdot 10^{-15}$ cm^2; $k \sim 1 \cdot 10^{-10}$ cm^3/s
46	$Cs(6P_{1/2}) + Cu \rightarrow Cs + Cu(D_{3/2})$	$k \sim 1.819 \cdot 10^{-11}$ cm^3/s
47	Ion mobility Cs^+	$6.52 \times (2.7 \cdot 10^{19}/Ne) \times (0.026/T_{g0})$

References

1. T. Karras, USA patent No. 3831107. *"Cesium quenched copper laser,"* Priority of August 20, 1974.

2. V.K. Isakov, M.M. Kalugin, and S.V. Pavlov, in: *Proc. of Xth Siberian Spectroscopy Meeting* (Tomsk, 1981), p. 155.

3. N.S. Belokrinitskii, L.V. Voronyuk, O.A. Glushchenko, S.N. Ezhov, I.P. Pinkevich, I.I. Opachko, P.A. Selishchev, V.P. Tretjak, V.S. Shevera, and M.T. Shpak, *"Studying of kinetics and power parameters of* CuCs *laser,"* Preprint No. 6, Institute of Physics, AS of the Ukrainian SSR, Kiev (1988), 33 pp.

4. Yu. Masumura, T. Ishikawa, and H. Saitoh, Appl. Phys. Lett. **64**, No. 25, 3380–3382 (1994).

5. G.Marshall, *"Kinetically enhanced copper vapor laser,"* D. Phyll. Thesis, Oxford (2003), 187 pp.

6. S. Sakata, K. Oohori, and M. Higuchi, IEEE J. Quant. Electron. **30**, No. 9, 2166–2172 (1994).

7. A. Ohzu, M. Kuto, and Y. Maruyama, Appl. Phys. Lett. **76**, No. 21, 2979–2981 (2000).

8. S.P. Bogacheva, L.V. Voronyuk, V.I. Lendjel, and A.M. Fedorchenko, Teplofizika Vysokikh Temperatur, No. 1, 11–16 (1983).

9. G.G. Petrash, Proc. SPIE **4747**, 193–197 (2002).

10. O.V. Zhdaneev and G.S. Evtushenko, Atmos. Oceanic Opt. **15**, No. 3, 207–212 (2002).

11. A.M. Boichenko and S.I. Yakovlenko, Kvant. Elektron. **32**, No. 2, 172–178 (2002).

12. A.M. Boichenko and S.I. Yakovlenko, Laser Phys., No. 7, 1007–1021 (2002).

13. A.M. Boichenko, G.S. Evtushenko, O.V. Zhdaneev, and S.I. Yakovlenko, Kvant. Elektron. **33** (2003) (in print).

14. A.M. Boichenko, G.S. Evtushenko, S.I. Yakovlenko, and O.V. Zhdaneev, Laser Phys. **12** (2003), (in print).

15. A.A. Radtsig and B.M. Smirnov, *Reference Book on Atom and Molecular Physics* (Atomizdat, Moscow, 1980), 240 pp.

16. V.I. Derzhiev, A.G. Zhidkov, and S.I. Yakovlenko, *Ion Emission in a Dense Medium* (Energoatomizgat, Moscow, 1986), 160 pp.

17. N.A. Lyabin, A.D. Chursin, and M.S. Domanov, Izv. Vyssh. Uchebn. Zaved., Ser. Fiz., No. 8, 67–73 (1999).

18. S.I. Yakovlenko, ed., *Visible and Near UV Plasma Lasers*, (Nauka, Moscow, 1989), 142 pp.

19. A.M. Boichenko, V.F. Tarasenko, and S.I. Yakovlenko, Laser Phys. **10**, No. 6, 1159–1187 (2001).

20. P.A. Bokhan, *"Metal vapor lasers with collisional deexcitation of lower working states,"* Doct. Phys.-Math. Sci. Dissert., Novosibirsk (1988), 418 pp.

21. S.I. Yakovlenko, Kvant. Elektron., No. 6, 501–505 (2000).

22. A.M. Boichenko, G.S. Evtushenko, S.I. Yakovlenko, and O.V. Zhdaneev, Laser Phys. **11**, No. 5, 580–588 (2001).

23. R.G. Garman, M.J. Withford, D.J.W. Brown, and J.A. Piper, Opt. Commun. **157**, December, 99–104 (1998).

24. A.N. Mal'tsev, *"Kinetics of repetitively pulsed generation of copper vapor laser,"* Preprint No. 1, Institute of Atmospheric Optics SB AS USSR, Tomsk (1982), 40 pp.